Pharmacological modulation of dopamine D1 and D2 receptors reveals distinct neural networks related to probabilistic learning in non-human primates.

Atsushi Fujimoto[1,2#]*, Catherine Elorette[1,2#], Satoka H. Fujimoto[1,2], Lazar Fleysher[5], Peter H. Rudebeck[1,2+], and Brian E. Russ[1,3,4+*]

Author affiliations:

[1] Nash Family Department of Neuroscience and Friedman Brain Institute, Icahn School of Medicine at Mount Sinai, One Gustave L. Levy Place, New York, NY 10029

[2] Lipschultz Center for Cognitive Neuroscience, Icahn School of Medicine at Mount Sinai, New York, NY, 10029

[3] Center for Biomedical Imaging and Neuromodulation, Nathan Kline Institute, 140 Old Orangeburg Road, Orangeburg, NY 10962

[4] Department of Psychiatry, New York University at Langone, One, 8, Park Ave, New York, NY 10016

[5] BioMedical Engineering and Imaging Institute, Icahn School of Medicine at Mount Sinai, One Gustave L. Levy Place, New York, NY 10029

[#] These authors contributed equally to this work

[+] Joint last author

*** Correspondence:**

Atsushi Fujimoto and Brian E. Russ

atsushi.fujimoto@mssm.edu or brian.russ@nki.rfmh.org

Acknowledgments

A.F., C.E., B.E.R., and P.H.R. are supported by grants from the BRAIN initiative (R01MH117040). B.E.R. is supported by grants from NIMH (R01MH111439) and NINDS (R01NS109498). A.F. is supported by Overseas Research Fellowship from Takeda Science Foundation and a Brain & Behavior Research Foundation Young Investigator grant (#28979). We would like to thank Dr. Paula Croxson for providing the foundation on which this work was built, Dr. Yukiko Hori for advising on drug preparation, and Jairo Muñoz and Niranjana Bienkowska for assistance with data acquisition. For help with fMRI data pre-

processing and analysis we thank Drs Paul Taylor and Alex Franco, respectively. We also thank Drs. Jacqueline-Marie Ferland and Takafumi Minamimoto for their comments on the earlier version of the manuscript.

Conflict of interest

The authors declare no competing financial interest.

Abstract

The neurotransmitter dopamine (DA) has a multifaceted role in healthy and disordered brains through its action on multiple subtypes of dopaminergic receptors. How modulation of these receptors controls behavior by altering connectivity across intrinsic brain-wide networks remains elusive. Here we performed parallel behavioral and resting-state functional MRI experiments after administration of two different DA receptor antagonists in macaque monkeys. Systemic administration of SCH-23390 (D1 antagonist) disrupted probabilistic learning when subjects had to learn new stimulus-reward associations and diminished functional connectivity (FC) in cortico-cortical and fronto-striatal connections. By contrast, haloperidol (D2 antagonist) improved learning and broadly enhanced FC in cortical connections. Further comparison between the effect of SCH-23390/haloperidol on behavioral and resting-state FC revealed specific cortical and subcortical networks associated with the cognitive and motivational effects of DA, respectively. Thus, we reveal the distinct brain-wide networks that are associated with the dopaminergic control of learning and motivation via DA receptors.

Introduction

Dopamine (DA), a neurotransmitter in the central nervous system, plays a critical role in cognition and action [1, 2, 3]. Specifically, DA is essential for normal patterns of learning, cognitive control, and working memory as well as motivated behavior [4, 5, 6, 7]. DA acts through its binding to various dopamine receptors that are heterogeneously distributed across the brain [8, 9]. The dopamine D1 and D2 receptors are the most prevalent subtypes of receptors in both humans and animals and they are heavily implicated in psychiatric conditions such as schizophrenia [10, 11].

Extensive research has found that D1 and D2 receptors have distinct roles in aspects of learning and motivation. For instance, systemic or local administration of dopaminergic agents in prefrontal cortex that block D1 receptors disrupts cue-reward association learning and probabilistic reversal learning in rats, while blocking of D2 receptors promotes learning [12, 13, 14, 15]. Similarly, studies using macaque monkeys found that local administration of a D1 antagonist, SCH-23390, into dorsolateral prefrontal cortex impaired working memory and learning [16, 17], while systemic administration of the D2 antagonist haloperidol, which is widely used to ameliorate positive symptoms of schizophrenia [18, 19], facilitated value discounting [20]. Besides the prior studies reporting the effects of DA receptor modulation on behavior, neuroimaging studies in healthy human subjects have reported that SCH-23390 induces deficits in working memory and that this effect on behavior is associated with reduced fronto-parietal fMRI functional connectivity [21]. Similarly, D2 antagonists haloperidol or amisulpride improve associative memory recall and shift decision thresholds in reinforcement learning and this is associated with enhanced reward-related signals in frontal and striatal areas [22, 23, 24, 25]. Taken together, these studies indicate that D1 and D2 receptor modulation causes different effects on behavior through distinct brain networks. Despite this, exactly which brain-wide networks of areas are affected by D1 and D2 receptor modulation and how those networks are associated with the behavioral effects remain unclear.

As noted above, a number of studies in humans have looked at the effects of D1 or D2 receptor modulation on behavior and fMRI functional connectivity. However, the extent to which modulation of DA receptors causes changes in intrinsic brain-wide functional connectivity has yet to be fully determined. One scenario is that the manipulation of specific DA receptor subtypes has an impact only on neural activity in the brain areas where the receptors are located [20, 26, 27, 28]. Alternatively, it is possible that manipulation of DA receptors more globally influences the patterns of networks of distributed brain areas by modulating neural activity in direct and indirect pathways in the cortico-basal ganglia circuits [29, 30]. Previous resting-state neuroimaging studies with pharmacological challenges have produced equivocal effects on neuroimaging assessments. Earlier PET and SPECT studies reported that the D2 antagonist haloperidol increases cerebral blood flow in healthy subjects and in clinically responsive schizophrenia patients [31, 32]. Resting-state fMRI studies showed a decrease in the hemodynamic response following administration of D1 antagonist SCH-23390 in rats [33], while either D2 antagonist haloperidol or bromocriptine enhanced dorsal fronto-parietal networks in healthy human subjects [34, 35]. Although these studies provided partial evidence as to how D1 and D2 modulation impacts brain-wide intrinsic MRI functional connectivity, the majority of these studies used low doses of these dopaminergic antagonists. This leaves open the question of how higher doses that are sufficient to robustly modulate behavior would impact brain-wide networks of functionally connected areas.

To address these issues, we conducted parallel behavioral and resting-state functional neuroimaging experiments in macaque monkeys. Macaques are a suitable model for this research as they have dopaminergic neural circuits that are comparable to humans [36, 37], and allow us to interrogate their brain-wide fMRI signal while we administer DA receptor antagonists at doses that are sufficient to

modulate behavior. Here we used SCH-23390 and haloperidol to modulate D1 and D2 receptors respectively. We specifically chose to assess the effects of haloperidol regarding D2 function on behavior and resting-state brain activity as it has been extensively used in prior works and continues to be used to treat schizophrenia. Thus, what we find has the potential to reveal brain-wide networks modulated by D1 and D2 receptors as well as having direct clinical relevance. We found that the D1 and D2 receptor selective antagonists, SCH-23390 and haloperidol respectively [38], induced contrasting effects on both behavior and functional connectivity in cortico-cortical and cortico-striatal networks. Further, the cortical functional connectivity changes induced by DA antagonists were correlated with task performance, especially when subjects had to learn new stimulus-reward associations. By contrast, changes in subcortical functional connectivity were more closely associated with DA antagonist-induced changes in response latency, an index of the subject's motivational state [39]. Thus, our results reveal the brain-wide impact of manipulating activity at specific DA receptors, shedding light on the neural networks that are associated with dopamine receptor-dependent cognitive function.

Results

Distinct effects of dopamine receptor antagonists on probabilistic stimulus-reward learning

Four macaque monkeys (Ee, Me, Pi, St) were trained to perform a probabilistic learning task for fluid rewards. On each trial, following an inter-trial interval (ITI) and fixation period, two visual stimuli were presented to the left and right of the screen. The animals were free to choose between the stimuli by making an eye movement to obtain a juice reward (**Fig. 1A**). The visual stimuli presented on each trial were randomly chosen from a set of three stimuli that were associated with distinct probabilities of receiving a juice reward (0.9, 0.5, and 0.3) (**Fig. 1B**). Subjects completed 100-trial blocks with either stimuli that they had previously learned (referred to as familiar blocks) or that were novel at the start of each block (referred to as novel blocks). Thus, in familiar blocks subjects should be able to maintain a high level of performance whereas in the novel blocks, subjects had to learn which stimulus was the most likely to lead to reward. The novel and familiar blocks were intermingled and the subjects completed 2-3 of each block type in a daily session. To assess the effects of pharmacological manipulation with dopamine receptor antagonists in this task, either SCH-23390 (D1 receptor antagonist), haloperidol (D2 receptor antagonist), or 0.9% saline was systemically (i.m.) administered in advance of the testing. The dosage of each drug was determined to achieve 50-80% occupancy of D1 and D2 receptors in macaques, respectively [20]. To ensure that there were no lasting effects of the drug, appropriate washout periods were included between injections (see Methods).

In blocks where the reward probabilities associated with novel stimuli had to be learned in the absence of either drug (i.e., saline sessions), monkeys gradually learned to discriminate between the different stimuli (**Fig. 1C**). By contrast, in the familiar blocks subjects reliably maintained a high and stable performance throughout a given block, suggesting that they were using previous learning to guide their choices (**Fig. 1E**). A two-way repeated-measures ANOVA (trial bin: 1-10 × block type: novel or familiar) revealed a significant interaction of trial bin by block type on choice performance ($p < 0.01$, $F_{(9,1097)} = 8.0$), confirming the difference between novel and familiar blocks.

Subjects' choice performance was also influenced by which stimuli were presented as options on each trial. A one-way repeated-measures ANOVA (stimulus pair: 0.9-0.3, 0.9-0.5, 0.5-0.3) revealed a

significant main effect of stimulus pair on choice performance in both novel and familiar blocks (novel blocks: $p < 0.01$, $F_{(2,168)} = 16.3$; familiar blocks: $p < 0.01$, $F_{(2,153)} = 15.3$, **Fig. 1C and E**). Additionally, response time (RT) reflected the reward probability of available options in both block types, such that RT was shorter for trials in which the high reward probability stimulus was presented (novel blocks: $p = 0.027$, $F_{(2,168)} = 3.7$; familiar blocks: $p < 0.01$, $F_{(2,153)} = 53.8$, main effect of stimulus pair, 1-way repeated-measures ANOVA, **Fig. 1D and F**). Importantly, the patterns of behavior were consistent across all subjects in both the novel and familiar blocks (**Fig. S1**).

Following dopamine receptor antagonists administration, behavioral performance was impacted (**Fig. 2**). Notably, we found that SCH-23390, our D1-receptor antagonist, tended to decrease subjects' ability to correctly discriminate the stimulus associated with the higher reward probability in novel blocks ($p = 0.061$, $F_{(3,441)} = 2.5$, main effect of drug dose, 2-way repeated-measures ANOVA), while it did not affect the performance in blocks with familiar stimuli ($p = 0.90$, $F_{(3,399)} = 0.20$) (**Fig. 2A**). Performance, depending on the drug dosage, followed an inverted U shape pattern where the low and high doses increased and decreased performance, respectively, in novel blocks. The treatment also affected RT such that higher doses of SCH increased RT in both novel and familiar blocks (novel blocks: $p < 0.01$, $F_{(3,441)} = 24.0$; familiar blocks: $p = 0.015$, $F_{(3,399)} = 3.5$) (**Fig. 2B**). Thus, D1 receptor antagonism appeared to have a selective effect on new associative learning in macaques as opposed to maintaining choices to learned associations.

In contrast to SCH-23390, haloperidol, our D2-receptor antagonist significantly increased subjects' ability to discriminate the novel stimuli associated with the highest probability of receiving a reward ($p = 0.037$, $F_{(2,342)} = 3.3$). Further, this effect was specific to novel blocks as opposed to the familiar blocks ($p = 0.63$, $F_{(2,309)} = 0.46$) (**Fig. 2C**). Notably, administration of haloperidol did not affect subjects RTs in either novel or familiar blocks ($p > 0.53$) (**Fig. 2D**). This latter finding indicates that the effect of D2 receptor antagonism is specific to cognitive aspects of the task at the range of doses we used, as opposed to altering monkeys' motivation to seek and receive rewards. Thus, dopamine receptor antagonists induced opposing effects on learning novel probabilistic stimulus-reward associations at the higher doses that we used, while they had no discernable impact on familiar associations.

Contrasting effects of dopamine receptor antagonists on fronto-striatal functional connectivity

Despite a rich literature demonstrating behavioral effects by DA receptor manipulation, studies demonstrated their effects on resting-state neural networks at the dosage high enough to induce clear behavioral effects have been lacking. Given the clear differences between D1 and D2 receptor antagonism on monkeys' performance of the probabilistic task, we next set out to determine which networks might be most influenced by our two DA receptor antagonists and therefore potentially driving the behavioral effects. To do this we analyzed resting-state functional images that were obtained in parallel to the behavioral experiments. The scans were conducted using the same protocol we previously employed [40, 41], where subjects are maintained on a light level of anesthesia (0.7-0.9% isoflurane) throughout a scan. We have found that this protocol robustly preserves functional connectivity (FC) in resting-state networks while minimizing motion-related artifacts. The resting-state images were collected both before and after drug injection (50 µg/kg SCH-23390, 10 µg/kg haloperidol, or saline, i.v.) where the pre-injection scans

served as a within-session baseline to control the session-by-session fluctuation of resting-state FCs. In addition to the cohort that completed behavioral testing detailed above, three additional macaques (monkeys Bu, Cy, Wo) also underwent scans where saline was injected after the pre-injection baseline period. Data from these animals serve as additional baseline data for our analyses (see **Table 1**).

First, to assess the effects of the drugs on an area known to be high in D1 and D2 receptors that has also been implicated in associative learning [42], we analyzed the change in FC of dorsal striatum induced by administration of either SCH-233980 or haloperidol. Here we used an ROI seed approach (ROI: dorsal striatum, SARM Level 4 atlas) [43]. During baseline imaging, before the injection of either drug, signal in dorsal striatum ROI exhibited high levels of correlation with frontal cortex, including parts of ventrolateral prefrontal cortex (vlPFC) and orbitofrontal cortex (OFC), areas that have been implicated in probabilistic learning [44, 45] (**Fig. 3A**). To assess the changes induced by pharmacological treatment, the pre-injection, baseline activity map of FC was subtracted from post-injection FC map for each treatment condition. As expected, injection of saline had little effect on dorsal striatum FC with the rest of the brain (**Fig. 3B**). By contrast, administration of SCH-23390 induced broad changes in dorsal striatum FC (**Fig. 3C**). Notably, D1-receptor antagonism specifically decreased dorsal striatum FC with OFC and lateral prefrontal cortex, while increasing correlations within the dorsal striatum itself. By contrast, administration of haloperidol significantly increased FC in frontal-striatal circuits, most notably in parts of the medial OFC and vlPFC (**Fig. 3D**), while showing minimal change in FC within the dorsal striatum. Thus, D1 and D2 receptor antagonism appears to have opposing effects on dorsal striatum FC in macaques, especially with the parts of frontal cortex involved in probabilistic learning.

Functional connectome analysis reveals distinct network signatures associated with dopamine receptor antagonism

To further characterize the impact of the D1 and D2 receptor antagonists on the brain-wide networks beyond the striatum, we performed atlas-based full connectome analyses. Here we use pre-determined anatomical ROIs from the cortical and subcortical atlas of the macaque monkey (CHARM and SARM atlas, respectively) [43, 46] and normalized FCs (z-value) were computed for all ROI pairs to produce connectomes. The pre-injection connectomes were similar to that reported previously [40, 47] (**Fig. 4A, left column**). Pre-injection connectomes were then subtracted from post-injection connectomes (**Fig. 4A, middle column**) to assess the impact of drug treatments (ΔFCs, **Fig. 4A, right column**). As expected, injections of saline were not associated with systematic changes in FCs of the cortical and subcortical connectome (**Fig. 4A, top row**). By contrast, SCH-23390 injection induced an overall decrease in FCs primarily between cortical regions (**Fig. 4A, middle row**), whereas haloperidol injection induced the opposite pattern of effects on FCs (**Fig. 4A, bottom row**). Indeed, the average z-value for each pair of ROIs showed contrasting effects overall, where SCH-23390 decreased and haloperidol increased FC between cortical sites ($p < 0.05$ with Bonferroni correction, rank-sum test, **Fig. 4B**).

We further visualized the changes in FC following injections of SCH-23390 or haloperidol by projecting the ΔFC connectomes onto circular plots (absolute difference in z-value > 0.1, **Fig. 4C**). This approach revealed unique patterns of network-level effects induced by SCH-23390 and haloperidol. Specifically, SCH-23390 was associated with a general decrease in cortical-cortical FC in frontal and

temporal areas, fronto-striatal FC, and meso/thalamo-cortical FCs. In contrast, haloperidol primarily caused an increase in cortico-cortical FC in frontal, parietal, and temporal areas as well as fronto-striatal FC. Overall, mirroring our earlier analyses, SCH-23390 and haloperidol induced contrasting effects in brain-wide FCs, and in particular induced opposite effects in fronto-striatal and cortico-cortical FCs.

Network correlates of behavioral performance associated with dopaminergic function

The prior analysis shows that the behavioral effects of D1 and D2 receptor antagonism are associated with distinct changes in brain-wide FC. To directly compare behavioral and neuroimaging datasets, we next examined whether the pharmacologically induced changes in resting-state functional connectivity (ΔFC) are related to the effects on behavioral data, either correct performance or RT, that were obtained after the administration of matching doses of the same D1- and D2-antagonists. Correlations were computed using ΔFC within a specific pair of ROIs, across all drug conditions, and behavioral effects under the same drug conditions. This allowed us to assess whether changes in FC were predictive of changes in behavioral responses during a task, even though they were tested under different settings.

As before, we first focused specifically on connectivity between the dorsal striatum and parts of frontal cortex as well as subcortical structures known to be involved in probabilistic learning. Notably, we found that dorsal striatum-to-OFC (Walker's area 11/13) ΔFC was significantly correlated with the correct performance in novel blocks ($p < 0.01$, $r = 0.32$) (**Fig. 5A and B**), while there was no association between performance in the familiar blocks ($p = 0.96$) or RTs ($p > 0.38$) (**Fig. 5C**). The same pattern was seen between OFC-to-12m/o (rostral vlPFC) ΔFC and behavior where positive correlation was observed between the FC changes and the performance in the novel block ($p < 0.01$, $r = 0.34$) (**Fig. 5D-F**). This specific relationship between the functional connections and correct performance in novel blocks indicates that these connections may be involved specifically in learning rather than in the performance of the probabilistic task in general. By contrast, we found a distinct effect on connectivity between mediodorsal thalamus and caudal vlPFC (area 12o) as ΔFC between these structures showed almost no correlation with the animals' performance during the novel blocks ($p = 0.79$, $r = 0.03$), there was a significant negative correlation with performance during the familiar blocks ($p = 0.016$, $r = -0.30$) (**Fig. 5G and H**). However, ΔFC of this functional connection was related to subject's RTs in both conditions (novel blocks: $p < 0.01$, $r = -0.45$; familiar blocks: $p < 0.01$, $p = -0.41$) (**Fig. 5I**). Similarly, ventral striatum-to-midbrain ΔFC was also related to RT effects in both conditions ($p < 0.032$) and showed no significant association with correct performance ($p > 0.074$) (**Fig. 5J-L**). The strong negative correlation observed between ΔFC and the animals' RTs suggests that these connections are involved in such as motivation or motor control.

Next, we extended the approach described above and conducted a similar analysis on the full connectome of all ROI pairs and measures of behavior (**Fig. 6**). **Figure 6A** depicts the functional connections where we observed a strong correlation between ΔFC and task performance. The brain map indicates that the task performance in novel blocks was positively correlated to cortico-cortical and cortico-subcortical ΔFCs (**Fig 6A, left**). Interestingly, the pattern was strikingly different when we analyzed the familiar block; strong correlation was observed mainly in subcortical regions, while cortico-cortical ΔFCs were less correlated to the performance (**Fig 6A, right**). Illustration of the full correlation matrix further revealed the detail of these differences. There was a strong correlation between ΔFCs in

cortical areas including frontal, parietal, and temporal regions, as well as in these regions' functional connections to striatum, and correct performance in the novel blocks (**Fig. 6C, left**). In the familiar blocks, there were less strong correlations in cortical areas, although some functional connections, such as the connections between midbrain nuclei and thalamic areas including mediodorsal thalamus as well as the connections between sensory and motor cortices, were strongly correlated to the performance (**Fig. 6C, right**). Consequently, when we averaged connections based on their link between cortical and subcortical ROIs (cortico-cortical, cortico-subcortical, and subcortico-subcortical), we found a distinct pattern of connections that showed strong correlation to task performance in each block type ($p < 0.01$, $F_{(2,15000)} = 68.1$, interaction of area category by block type, 2-way ANOVA) (**Fig. 6E**). Subsequent post-hoc analysis revealed that the cortico-cortical and cortico-subcortical behavior-ΔFC correlations were higher in the novel blocks compared to familiar blocks ($p < 0.01$, Tukey-Kramer test), while the relationship between subcortico-subcortical ΔFC and behavioral performance was lower in novel blocks and higher in familiar blocks ($p < 0.01$) (**Fig. 6E**). Thus this analysis revealed distinct neural networks that are associated with learning performance and choice performance in familiar blocks, where the former is mainly in cortical areas and the latter involves more subcortical connections.

We performed a similar analysis between ΔFC and RT across novel and familiar blocks (**Fig. 6B and D**). Here we observed a negative correlation between behavior and ΔFC in cortical areas but a positive correlation between behavior and ΔFC in midbrain and thalamic connections in both novel and familiar blocks of trials. Consequently, we saw a similar pattern of connections across the two conditions (**Fig. 6F**) although there was a significant interaction of area category by block type ($p < 0.01$, $F_{(2,15000)} = 4.6$). Post-hoc analysis showed significant difference in cortico-cortical and cortico-subcortical connections between novel and familiar blocks ($p < 0.01$, Tukey-Kramer test), but no significant difference was observed in subcortico-subcortical connections ($p = 1.0$), suggesting RT was associated with subcortical FC in a similar manner in both blocks. Interestingly, the pattern of correlation between RT and ΔFC was similar to that with task performance in familiar blocks, although it is distinct from the network associated with the performance in novel blocks (**Fig. 6C and D**). This result suggests that the brain-wide networks associated with learning novel associations that are modulated by dopaminergic antagonists are largely separable from those associated with memory-based choices to familiar stimuli or RTs, in which behavioral variability was primarily associated with subcortical structures. We also conducted the same analysis with behavioral data normalized for each subject (z-transformed). The networks correlated to each behavior matched those shown in Figure 6; cortico-cortical and cortico-subcortical behavior-ΔFC correlations were higher in the novel blocks compared to familiar blocks ($p < 0.01$, Tukey-Kramer test) and subcortico-subcortical behavior-ΔFC correlations were lower in novel blocks than that in familiar blocks ($p < 0.01$). No significant difference in subcortico-subcortical connections was observed in the relationship between the RT and ΔFC ($p = 0.40$). In sum, our analysis directly correlating behavior and resting-state FC changes induced by dopaminergic receptor antagonists revealed distinct neural networks that were associated with specific behavioral domains.

Discussion

Here we conducted concurrent behavioral and resting-state fMRI experiments in macaque monkeys to assess the impact of dopamine D1 and D2 receptor antagonists on the brain-wide networks that support

learning and motivation. Administration of the D1 receptor antagonist SCH-23390 reduced performance when subjects had to learn novel stimulus-reward associations in a probabilistic learning task. By contrast, administration of the D2 receptor antagonist haloperidol improved performance on the same task. Neither drug affected performance when subjects had to choose between well-learned, familiar stimuli where choices were guided by prior knowledge about the association. Mirroring the effects on task performance, fMRI resting-state FC analysis revealed contrasting effects associated with the D1 and D2 receptor antagonism which were mainly confined to the cortico-cortical and fronto-striatal networks. When we looked for relationships between behavior and changes in FC induced by D1/D2 antagonists, we found that effects of dopaminergic manipulation related to learning were associated with cortico-cortical connections whereas the effect on the more motoric or motivational aspects of task performance were associated with subcortical FC. Taken together, our results identified distinct brain-wide networks that appear to underlie the impact of D1 and D2 antagonists on learning and motivation, respectively.

The role of D1 and D2 receptors in learning and memory-based choices

The effects of DA receptor manipulation on behavior have been extensively studied in both humans and animals. Past reports using rats showed that the administration of D1 antagonist SCH-23390 and D2 antagonist raclopride or eticlopride induced opposing effects in reward-based learning and probabilistic choices [12, 13, 14, 15]. Similarly, blocking prefrontal D1 receptors also impaired working memory in macaque monkeys [16, 17], and D2 antagonism enhanced reward-related signal and new association learning in healthy human subjects [23, 24, 25] and facilitated discounting of reward value with workload cost in macaque monkeys [20]. In addition to such cognitive roles, D1 and D2 stimulation alter sensory processing in prefrontal neurons [7, 48, 49] and responses to self-initiated motion [50]. Interestingly, unlike robust behavioral effects observed in past studies using animal subjects, recent studies using healthy human subjects demonstrated that D2 antagonist haloperidol did not induce a clear effect on exploration/exploitation behaviors in a reinforcement learning task [51], although the follow-up study by the same group found a consistent reduction of the decision threshold by the drug administration in the same paradigm [22]. These relatively mixed effects of D2 antagonists could be accounted for by the choice of dosages given to participants and potential individual variability in the baseline level of dopamine dependency [51]. To ensure a high enough proportion of DA receptors are blocked in individual animals, we chose our dosage of antagonists based on a prior study that established the DA receptor occupancy of SCH and haloperidol using PET imaging in macaques [20]. With this information in hand, we were able to block the receptors at pharmacologically effective levels.

Our behavioral results using macaque monkeys as subjects were overall consistent with the existing literature; D1 antagonist SCH impaired and D2 antagonist haloperidol facilitated the performance of our monkeys when they had to learn new associations (**Fig. 2**). Notably, DA receptor manipulation in this range did not affect the performance in the familiar block where the animals were choosing between known options, suggesting that the action of DA through D1 and D2 receptors play a specific role in new association learning rather than choice actions in general. In addition to the effects on learning, we observed the change in response time specifically in the sessions where SCH was administered but not in haloperidol sessions. Notably the impact of SCH on RT was linear and observed in both novel and familiar

blocks, unlike the effects on the correct performances, suggesting this effect on motivation or motor function is likely to be dissociable from the effects on learning.

Dopaminergic modulation of fMRI resting-state functional connectivity

G protein-coupled D1 and D2 receptors mediate distinct molecular signaling when DA attaches to them by coupling to G_s or $G_{i/o}$, class of α subunit, respectively [38]. Previous studies have mainly analyzed neural data by focusing on specific areas such as prefrontal cortex and striatum [7, 16, 50, 52, 53], thus the effects of DA receptor manipulation at the whole-brain level remained less clear. Further, one advantage of our anesthetized resting-state fMRI with pharmacological challenge approach is that it can identify drug effects on intrinsic networks free from the indirect impact of drug-induced behavioral changes as is often done in neuroimaging studies in humans. We previously developed a neuroimaging protocol that uses a low level of anesthesia that is able to preserve resting-state FC at the whole-brain level in macaque monkeys that is also sensitive to pharmacological treatment on brain-wide FC pattern [40, 41]. Here we took this approach and extended it to assess the impact of high-dose D1 and D2 antagonists in the brain of macaques. The whole-brain connectome approach revealed contrasting impacts of SCH and haloperidol, particularly in cortico-cortical and cortico-subcortical connections, mirroring the decrease and increase in learning performance induced by the same drugs (**Fig. 4**). In addition to the known effects on fronto-striatal circuit and fronto-parietal network, diverse cortical areas including temporal areas were involved. Also SCH strongly modulated thalamo-cortical FCs. The present result highlighted that the large-scale networks were recruited to influence various cognitive and motor functions.

Interestingly, this pattern of DA receptor manipulation by each receptor antagonist did not simply reflect the known distribution of these receptor subtypes within the primates' brain (**Fig. 4**). Previous PET studies showed that D1 receptors are widely expressed in both cortical and subcortical areas whereas D2 receptors are localized in subcortical areas such as the striatum and only sparsely expressed in cortical areas in both humans and macaques [20, 26, 27, 28]. With this in mind, one scenario is that the D2 receptor manipulation mainly affects subcortical FCs. However, what we observed in the present study was that haloperidol induced marked changes in cortical FCs, suggesting a complementary mechanism by which D2 manipulation alters cortical functional communication. It is unlikely that the non-specific binding of haloperidol to D1 receptors caused changes in cortical areas, as the overall direction of the behavioral and neural effects was the opposite between those drug conditions. One possibility is that the D2 antagonist induced substantial neural changes in cortical regions through interactions with D2 receptors expressed in cortical neurons [38]. Indeed, previous studies demonstrated that cortical D2 receptors were functionally relevant [54, 55] and their density in prefrontal areas was associated with the severity of positive symptoms in patients with schizophrenia [56, 57], although the profile of cortical D2 receptors is still unclear due to remaining technical limitations [58]. Another possibility is that the antagonism to the DA receptors in the striatum, where D1 and D2 receptors are expressed mainly in direct and indirect pathway medium spiny neurons (MSNs), respectively, activated either pathway to modulate activity across areas and thereby alter FC within cortical areas [29, 30]. Interestingly, a previous study demonstrated that systemic administration of haloperidol suppressed neuronal firing of MSNs and enhanced firing of striatal interneurons, which could lead to excitation of frontal circuits through disinhibition of indirect pathway [52]. Although our data do not provide the exact mechanism by which D1 and D2 receptor antagonists induce their effects, we do provide

direct evidence that these antagonists lead to opposite patterns of brain-wide changes in FC. Future studies could identify the exact mechanisms through which DA receptor manipulation induces brain-wide changes by recording neuronal activity from D1 and D2 receptor expressing neurons in both cortical and striatal regions.

Dissociable neural networks for distinct dopamine-dependent behaviors

Past studies have demonstrated that resting-state fMRI measures of FC can predict behavioral effects of pharmacological treatments on cognitive tasks that assess learning, memory recall, and attention, in both humans and macaques [40, 59, 60]. That the effects of DA receptor manipulation on resting-state fMRI could predict the pattern of behaviors in probabilistic learning and choice responses fits with this prior literature. Further, our within-subject design, with parallel behavioral and resting-state fMRI experiments, allowed us to directly compare DA receptor manipulation effects on cognitive behaviors and intrinsic neural network dynamics. The behavior-connectome correlation analysis revealed distinct pattern of neural networks that were correlated to task performance or RT (**Fig. 6**). Previous studies have shown that the interaction between frontal cortex and striatum is vital for cognitive control and reinforcement learning [61, 62]. In addition, a wide variety of cortico-cortical interactions including fronto-parietal network has been implicated in learning and memory formation [63, 64]. Interestingly, the learning-related network revealed by our behavior-connectome analysis appeared to be largely overlapped onto such known neural networks that are active when subjects are engaging in reward-based association learning [65, 66], suggesting that our dopaminergic receptor manipulation triggered changes in neural dynamics around the neural network that are relevant to task performance even at rest, which may guide behaviors when subjects are awake and engaging a task.

It is noteworthy that the network reflecting task performance in familiar blocks is largely different from the network correlated with novel block performance, as they involved less cortical connections and more subcortical connections most prominently around midbrain and thalamic nuclei (**Fig. 5 and 6**). Interestingly, significant involvement of subcortical connections was also observed in the neural network correlated with RT, suggesting similarity between the neural networks across different behavioral domains. Considering such a similar pattern across different behavioral domains emerged, this subcortical network may play a crucial role in motivation or motor control, which contributes to choice execution in general. Interestingly, dopaminergic innervation of thalamic nuclei such as the mediodorsal thalamus is particularly prominent in primate species compared to rodents [67, 68] and its function is implicated in psychosis in schizophrenia [69, 70]. Thus, our analysis revealed distinct neural networks that are associated with learning and cognitive control, which may highlight the neural networks where dopamine takes action to modulate behaviors in primates.

Conclusion and relation to mental health

The bidirectional changes induced by D1 and D2 antagonists at both behavioral and neural levels implicated that the maintenance of optimal balance between D1 and D2 receptor-dependent DA signaling is critical to normal learning [8, 71], which is potentially distorted in psychiatric conditions implicated in

dopaminergic malfunction such as schizophrenia [72]. Indeed, recent studies pointed out that the balance of effects onto D1 and D2 receptors could be a critical factor that determines the efficacy of an anti-psychotic drug [73]. Given the similarity of DA system between non-human primates and humans [36, 37], the current results may implicate the altered DA system in psychiatric diseases and the mechanisms through which pharmacological DA receptor manipulation ameliorates the aberrant behaviors.

Methods

Subjects

Seven rhesus macaques (*Macaca mulatta,* 7-8 years old, 4 females) served as subjects. A subset of four monkeys (monkeys Ee, Me, Pi, St) underwent behavioral testing with pharmacological challenge. All monkeys underwent resting-stated fMRI scans for at least one treatment condition. The experiments performed for each subject are summarized in **Table 1**. All procedures were reviewed and approved by the Icahn School of Medicine Animal Care and Use Committee.

Surgery

Prior to training, an MRI compatible head-fixation device (Rogue research) was surgically implanted using dental acrylic (Lang Dental, Wheeling, IL) and ceramic screws (Thomas Research Products, Elgin, IL) in the animals that underwent behavioral testing (monkeys Ee, Me, Pi, St). In a dedicated operating suite using aseptic procedures, anesthesia was induced using ketamine (5 m/kg) and dexmedetomidine (0.0125 mg/kg) and then maintained by isoflurane (2-3%). The skin, fascia, and muscles were opened and retracted. 8-10 screws were implanted into the cranium and the head fixation device was bonded to the screws using dental acrylic. The muscles, fascia, and skin were then sutured closed. The animals were treated with dexamethasone sodium phosphate (0.4 mg/kg, i.m.) and cefazolin antibiotic (15 mg/kg, i.m.) for one day before and one week after surgery. After surgery and for two additional days, the animals received ketoprofen analgesic (10-15 mg/kg, i.m.); ibuprofen (100 mg) was administered for five additional days and all postoperative medications were given in consultation with veterinary staff. The position of implant was determined based on a pre-acquired T1-weighted MR image.

Drugs

SCH-23390 hydrochloride (Tocris Bioscience, Minneapolis, MN) and haloperidol (Sigma-Aldrich, St. Louis, MO) were used as our D1 and D2 receptor selective antagonists, respectively. Both SCH and haloperidol were dissolved and diluted in 0.9% saline to achieve target dose of 1 ml solution. 0.9% saline (1 ml) was also used as a control solution. The solution was prepared fresh on every experimental day.

Probabilistic learning task

A reward-based probabilistic learning task was developed for macaque monkeys. The task was controlled by NIMH MonkeyLogic software [74] running on MATLAB 2019a (MathWorks, Natick, MA) and presented on a monitor in front of the monkey. In this task, animals were required to choose between two visual stimuli that were presented on a monitor using eye movements to signal their choices. A trial began with appearance of a fixation spot (white cross) at the center of a screen in front of a monkey. The monkey had to move the eyes toward the cross and maintain fixation for 1-1.5 sec to initiate a trial. Then the fixation spot was extinguished and visual stimuli were simultaneously presented to the right and left on the screen. The two stimuli presented on each trial were randomly chosen from a larger pool of three visual

stimuli that were associated with different reward probabilities (0.9, 0.5, and 0.3). Each trial therefore fell into three categories based on the reward probabilities of the options presented: High-Low (0.9-0.3), High-Medium (0.9-0.5), and Medium-Low (0.5-0.3). Stimuli were either novel at the beginning of each block of 100 trials (novel block) or subjects had previously learned about the probability of receiving a reward associated with each image and were highly familiar with them (familiar block). Once stimuli were presented, subjects were required to move their eyes toward either right or left stimulus option ('response') within 2 seconds. Following a response, the chosen stimulus remained on screen for 0.3 sec and then was removed, and a reward (1 drop of apple juice) was provided in accordance with the probability of the chosen option. Subsequently an inter-trial interval (ITI, 3-3.5 sec) followed. A trial with a fixation break during the fixation period or with no response within the response window was aborted; all stimuli were extinguished immediately and ITI started. The same trial was repeated following an aborted trial.

The animals performed 4-6 blocks in which the novel or familiar stimuli were pseudorandomly interleaved in hour-long sessions. The monkeys were trained for 3-6 months before behavioral experiment with drug injections or resting-state fMRI scans. The injection of saline, SCH-23390, or haloperidol solution (i.m.) was performed 15 minutes prior to the task start [20]. The order of treatment was randomized, and the injection was at least a day apart (SCH-23390) or a week apart (haloperidol) to avoid potential prolonged effects of the drug, in accordance with known pharmacokinetics of the drugs in macaque monkeys [20].

Behavioral data analyses

All behavioral data was analyzed using MATLAB 2019a. Choice performance was defined as the proportion of trials in a block (100 trials) in which monkeys chose an option associated with higher reward probability in the stimulus pair presented. Response time (RT) was defined as the duration from the timing of visual stimuli presentation to the timing of response initiation. Choice performance was computed for bins of 10 trials at each block and averaged for each subject, then finally averaged across subjects for each block type. We reasoned that a significant interaction ($p < 0.05$) of trial bin by block type with 2-way repeated measures ANOVA (trial bin: 1-10 × block type: novel or familiar) indicated that there was an improvement in performance due to successful learning in novel blocks but not in familiar blocks. Choice performance and RT on each stimulus pair in the latter half of each block were assessed by 1-way repeated-measures ANOVA (stimulus pair: 0.9-0.3, 0.9-0.5, 0.5-0.3) for each block type in saline sessions. The effect of SCH-23390 or haloperidol injection on choice performance and RT was assessed by 2-way repeated-measures ANOVA (stimulus pair: 0.9-0.3, 0.9-0.5, 0.5-0.3 × dose: 0, 10, 30, 50 μg/kg for SCH-23390, and 0, 5, or 10 μg/kg for haloperidol, respectively). Monkeys were modeled as a random effect.

Resting-state fMRI data acquisition

The scans were performed under the same protocol we previously developed for macaque monkeys [40, 41]. In brief, following sedation with ketamine (5mg/kg) and dexmedetomidine (0.0125mg/kg) the animals were intubated. They were then administered (i.v.) monocrystalline iron oxide nanoparticle or MION (10 mg/kg, BioPAL, Worcester, MA), and three EPI functional scans (1.6 mm isotropic, TR/TE 2120/16 ms, flip angle 45°, 300 volumes per each run) were obtained, along with a T1-weighted structural scan (0.5 mm isotropic, MPRage TR/TI/TE 2500/1200/3.27 ms, flip angle 8°) (pre-injection scans). Following drug i.v. injection (saline, SCH-23390, or haloperidol) and 15 minutes waiting period, another set of three functional scans was acquired (post-injection scans). Low-level isoflurane (0.7-0.9%) was used to maintain sedation through a session so that neural activity was preserved while minimizing motion artifacts. The doses of drugs used in the scans (50 μg/kg and 10 μg/kg for SCH and haloperidol, respectively) were the highest doses used in the behavioral experiment that reliably induced behavioral

effects in the novel blocks (see **Fig. 2**). Vital signs (end-tidal CO_2, body temperature, blood pressure, capnograph) were continuously monitored and maintained as steadily as possible throughout an experimental session.

fMRI data analysis

The detail of preprocessing steps for functional imaging data was described in our previous study [40]. In brief, all functional imaging data was initially converted to NIFTI format and preprocessed with custom AFNI/SUMA pipelines [40, 46, 75]. The T1 weighted image from each session was skullstripped [76] and then warped to the standard NMT atlas space [77]. The EPI data were further preprocessed using a customized version of the AFNI NHP preprocessing pipeline [46]. The first 3 TRs of each EPI were removed to eliminate any magnetization effects. Then, the images went through slice timing correction, motion correction, alignment to T1w image, warping to standard space, blurring, and then converted to percent signal change. Finally, motion derivatives from each scan along with CSF and WM signals were regressed and the residuals of this analysis were used in the following analysis.

The functional connectivity (FC) analysis was performed using 3dNetCorr function in AFNI [75, 78]. The regions of interest (ROIs) were defined based on the cortical hierarchical atlas (CHARM) [46] and subcortical hierarchical atlas (SARM) [43] for rhesus macaques, both at level 4. The matrices of FC across all ROI pairs, or connectomes, were Fisher's z-transformed for each session, and the pre-injection connectome was subtracted from post-injection connectome. Then, the connectomes representing the drug-induced change in FC (ΔFC) were averaged within treatment conditions (SCH-23390, haloperidol, saline). To statistically determine the effects, the ΔFCs derived from each ROI were averaged and compared to a null distribution ($\alpha = 0.05$ with Bonferroni's correction, rank-sum test). The connectomes were also visualized in the circular plot with threshold at $z = 0.1$ (absolute value) created using the circularGraph toolbox run in MATLAB [79].

The relationship between the connectome and behavioral data (correct performance and RT) was analyzed on the data where ΔFC and behavioral data were obtained under the same drug condition, and all drug conditions (saline, SCH, haloperidol) were combined. The correlation analysis was performed separately for each functional connection or ROI pair, and the matrix of correlation coefficient (R) was created. This matrix was also projected into a brain map of macaque monkeys by connecting the center of each ROI with a line reflecting the R-value and sign (positive or negative) of correlation as the line width and color, respectively. For visualization purposes the fraction of connections that showed strong behavior-ΔFC correlation (top 5%) were plotted. The R values in the matrix were averaged across functional connections for each of cortico-cortical, cortico-subcortical, and subcortico-subcortical ROI pairs and compared to the null distribution (rank-sum test).

References

1. Ott T, Nieder A. Dopamine and Cognitive Control in Prefrontal Cortex. *Trends in cognitive sciences* **23**, 213-234 (2019).

2. Robbins TW, Everitt BJ. Dopamine — Its Role in Behaviour and Cognition in Experimental Animals and Humans. In: *Dopamine in the CNS II* (ed Di Chiara G). Springer Berlin Heidelberg (2002).

3. Remy P, Samson Y. The role of dopamine in cognition: evidence from functional imaging studies. *Current Opinion in Neurology* **16**, S37-S41 (2003).

4. Brozoski TJ, Brown RM, Rosvold HE, Goldman PS. Cognitive deficit caused by regional depletion of dopamine in prefrontal cortex of rhesus monkey. *Science (New York, NY)* **205**, 929-932 (1979).

5. Volkow ND*, et al.* Association between decline in brain dopamine activity with age and cognitive and motor impairment in healthy individuals. *The American journal of psychiatry* **155**, 344-349 (1998).

6. Schultz W, Dayan P, Montague PR. A Neural Substrate of Prediction and Reward. *Science (New York, NY)* **275**, 1593-1599 (1997).

7. Noudoost B, Moore T. Control of visual cortical signals by prefrontal dopamine. *Nature* **474**, 372-375 (2011).

8. Seeman P. Dopamine receptors and the dopamine hypothesis of schizophrenia. *Synapse (New York, NY)* **1**, 133-152 (1987).

9. Self DW. Dopamine Receptor Subtypes in Reward and Relapse. In: *The Dopamine Receptors* (ed Neve KA). Humana Press (2010).

10. Lidow MS, Williams GV, Goldman-Rakic PS. The cerebral cortex: a case for a common site of action of antipsychotics. *Trends in pharmacological sciences* **19**, 136-140 (1998).

11. Brisch R*, et al.* The Role of Dopamine in Schizophrenia from a Neurobiological and Evolutionary Perspective: Old Fashioned, but Still in Vogue. *Frontiers in Psychiatry* **5**, (2014).

12. Eyny YS, Horvitz JC. Opposing roles of D1 and D2 receptors in appetitive conditioning. *The Journal of neuroscience : the official journal of the Society for Neuroscience* **23**, 1584-1587 (2003).

13. Jenni NL, Li YT, Floresco SB. Medial orbitofrontal cortex dopamine D(1)/D(2) receptors differentially modulate distinct forms of probabilistic decision-making. *Neuropsychopharmacology : official publication of the American College of Neuropsychopharmacology* **46**, 1240-1251 (2021).

14. St Onge JR, Abhari H, Floresco SB. Dissociable contributions by prefrontal D1 and D2 receptors to risk-based decision making. *The Journal of neuroscience : the official journal of the Society for Neuroscience* **31**, 8625-8633 (2011).

15. Zeeb FD, Robbins TW, Winstanley CA. Serotonergic and dopaminergic modulation of gambling behavior as assessed using a novel rat gambling task. *Neuropsychopharmacology : official publication of the American College of Neuropsychopharmacology* **34**, 2329-2343 (2009).

16. Puig MV, Miller EK. The role of prefrontal dopamine D1 receptors in the neural mechanisms of associative learning. *Neuron* **74**, 874-886 (2012).

17. Sawaguchi T, Goldman-Rakic PS. D1 dopamine receptors in prefrontal cortex: involvement in working memory. *Science (New York, NY)* **251**, 947-950 (1991).

18. Adams CE, Bergman H, Irving CB, Lawrie S. Haloperidol versus placebo for schizophrenia. *Cochrane Database of Systematic Reviews*, (2013).

19. Settle EC, Jr., Ayd FJ, Jr. Haloperidol: a quarter century of experience. *The Journal of clinical psychiatry* **44**, 440-448 (1983).

20. Hori Y*, et al.* D1- and D2-like receptors differentially mediate the effects of dopaminergic transmission on cost-benefit evaluation and motivation in monkeys. *PLoS biology* **19**, e3001055 (2021).

21. Fischer H*, et al.* Simulating neurocognitive aging: effects of a dopaminergic antagonist on brain activity during working memory. *Biological psychiatry* **67**, 575-580 (2010).

22. Chakroun K*, et al.* Dopamine regulates decision thresholds in human reinforcement learning in males. *Nature communications* **14**, 5369 (2023).

23. Clos M, Bunzeck N, Sommer T. Dopamine Enhances Item Novelty Detection via Hippocampal and Associative Recall via Left Lateral Prefrontal Cortex Mechanisms. *The Journal of neuroscience : the official journal of the Society for Neuroscience* **39**, 7920-7933 (2019).

24. Kahnt T, Weber SC, Haker H, Robbins TW, Tobler PN. Dopamine D2-receptor blockade enhances decoding of prefrontal signals in humans. *The Journal of neuroscience : the official journal of the Society for Neuroscience* **35**, 4104-4111 (2015).

25. Jocham G, Klein TA, Ullsperger M. Dopamine-Mediated Reinforcement Learning Signals in the Striatum and Ventromedial Prefrontal Cortex Underlie Value-Based Choices. *The Journal of Neuroscience* **31**, 1606-1613 (2011).

26. Tsukada H, Nishiyama S, Fukumoto D, Sato K, Kakiuchi T, Domino EF. Chronic NMDA antagonism impairs working memory, decreases extracellular dopamine, and increases D1 receptor binding in prefrontal cortex of conscious monkeys. *Neuropsychopharmacology : official publication of the American College of Neuropsychopharmacology* **30**, 1861-1869 (2005).

27. Suhara T*, et al.* Extrastriatal dopamine D2 receptor density and affinity in the human brain measured by 3D PET. *The international journal of neuropsychopharmacology* **2**, 73-82 (1999).

28. Froudist-Walsh S*, et al.* A dopamine gradient controls access to distributed working memory in the large-scale monkey cortex. *Neuron* **109**, 3500-3520.e3513 (2021).

29. Lee HJ*, et al.* Activation of Direct and Indirect Pathway Medium Spiny Neurons Drives Distinct Brain-wide Responses. *Neuron* **91**, 412-424 (2016).

30. Trantham-Davidson H, Neely LC, Lavin A, Seamans JK. Mechanisms underlying differential D1 versus D2 dopamine receptor regulation of inhibition in prefrontal cortex. *The Journal of neuroscience : the official journal of the Society for Neuroscience* **24**, 10652-10659 (2004).

31. Buchsbaum MS*, et al.* Striatal metabolic rate and clinical response to neuroleptics in schizophrenia. *Archives of general psychiatry* **49**, 966-974 (1992).

32. Goldman RG, Alexander GE, Zemishlany Z, Mukherjee S, Sackeim HA, Prohovnik I. Acute effects of haloperidol on cerebral cortex blood flow in normal and schizophrenic subjects. *Biological psychiatry* **40**, 604-608 (1996).

33. Choi JK, Chen YI, Hamel E, Jenkins BG. Brain hemodynamic changes mediated by dopamine receptors: Role of the cerebral microvasculature in dopamine-mediated neurovascular coupling. *NeuroImage* **30**, 700-712 (2006).

34. Vogelsang DA*, et al.* Dopamine Modulates Effective Connectivity in Frontal Cortex. *Journal of cognitive neuroscience*, 1-11 (2023).

35. Cole DM, Beckmann CF, Oei NYL, Both S, van Gerven JMA, Rombouts SARB. Differential and distributed effects of dopamine neuromodulations on resting-state network connectivity. *NeuroImage* **78**, 59-67 (2013).

36. Raghanti MA, Stimpson CD, Marcinkiewicz JL, Erwin JM, Hof PR, Sherwood CC. Cortical dopaminergic innervation among humans, chimpanzees, and macaque monkeys: A comparative study. *Neuroscience* **155**, 203-220 (2008).

37. Berger B, Gaspar P, Verney C. Dopaminergic innervation of the cerebral cortex: unexpected differences between rodents and primates. *Trends Neurosci* **14**, 21-27 (1991).

38. Beaulieu J-M, Gainetdinov RR. The Physiology, Signaling, and Pharmacology of Dopamine Receptors. *Pharmacological Reviews* **63**, 182-217 (2011).

39. Roesch MR, Olson CR. Neuronal Activity Related to Reward Value and Motivation in Primate Frontal Cortex. *Science (New York, NY)* **304**, 307-310 (2004).

40. Fujimoto A*, et al.* Resting-State fMRI-Based Screening of Deschloroclozapine in Rhesus Macaques Predicts Dosage-Dependent Behavioral Effects. *The Journal of neuroscience : the official journal of the Society for Neuroscience* **42**, 5705-5716 (2022).

41. Elorette C*, et al.* The neural basis of resting-state fMRI functional connectivity in fronto-limbic circuits revealed by chemogenetic manipulation. *bioRxiv*, (2023).

42. Clarke HF, Robbins TW, Roberts AC. Lesions of the medial striatum in monkeys produce perseverative impairments during reversal learning similar to those produced by lesions of the orbitofrontal cortex. *The Journal of neuroscience : the official journal of the Society for Neuroscience* **28**, 10972-10982 (2008).

43. Hartig R*, et al.* The Subcortical Atlas of the Rhesus Macaque (SARM) for neuroimaging. *NeuroImage* **235**, 117996 (2021).

44. Murray EA, Rudebeck PH. Specializations for reward-guided decision-making in the primate ventral prefrontal cortex. *Nature reviews Neuroscience* **19**, 404-417 (2018).

45. Rudebeck PH, Saunders RC, Lundgren DA, Murray EA. Specialized Representations of Value in the Orbital and Ventrolateral Prefrontal Cortex: Desirability versus Availability of Outcomes. *Neuron* **95**, 1208-1220.e1205 (2017).

46. Jung B*, et al.* A comprehensive macaque fMRI pipeline and hierarchical atlas. *NeuroImage* **235**, 117997 (2021).

47. Grayson DS*, et al.* The Rhesus Monkey Connectome Predicts Disrupted Functional Networks Resulting from Pharmacogenetic Inactivation of the Amygdala. *Neuron* **91**, 453-466 (2016).

48. Ott T, Stein AM, Nieder A. Dopamine receptor activation regulates reward expectancy signals during cognitive control in primate prefrontal neurons. *Nature communications* **14**, 7537 (2023).

49. Stalter M, Westendorff S, Nieder A. Dopamine Gates Visual Signals in Monkey Prefrontal Cortex Neurons. *Cell reports* **30**, 164-172.e164 (2020).

50. Kunimatsu J, Tanaka M. Striatal dopamine modulates timing of self-initiated saccades. *Neuroscience* **337**, 131-142 (2016).

51. Chakroun K, Mathar D, Wiehler A, Ganzer F, Peters J. Dopaminergic modulation of the exploration/exploitation trade-off in human decision-making. *eLife* **9**, (2020).

52. Yael D*, et al.* Haloperidol-induced changes in neuronal activity in the striatum of the freely moving rat. *Frontiers in systems neuroscience* **7**, (2013).

53. Wang M, Vijayraghavan S, Goldman-Rakic PS. Selective D2 receptor actions on the functional circuitry of working memory. *Science (New York, NY)* **303**, 853-856 (2004).

54. Narendran R*, et al.* Imaging dopamine transmission in the frontal cortex: a simultaneous microdialysis and [11C]FLB 457 PET study. *Molecular psychiatry* **19**, 302-310 (2014).

55. Narendran R*, et al.* Positron emission tomography imaging of amphetamine-induced dopamine release in the human cortex: a comparative evaluation of the high affinity dopamine D2/3 radiotracers [11C]FLB 457 and [11C]fallypride. *Synapse (New York, NY)* **63**, 447-461 (2009).

56. Suhara T*, et al.* Decreased dopamine D2 receptor binding in the anterior cingulate cortex in schizophrenia. *Archives of general psychiatry* **59**, 25-30 (2002).

57. Mizrahi R*, et al.* Adverse subjective experience with antipsychotics and its relationship to striatal and extrastriatal D2 receptors: a PET study in schizophrenia. *The American journal of psychiatry* **164**, 630-637 (2007).

58. Tritsch Nicolas X, Sabatini Bernardo L. Dopaminergic Modulation of Synaptic Transmission in Cortex and Striatum. *Neuron* **76**, 33-50 (2012).

59. Kohno M, Morales AM, Ghahremani DG, Hellemann G, London ED. Risky decision making, prefrontal cortex, and mesocorticolimbic functional connectivity in methamphetamine dependence. *JAMA psychiatry* **71**, 812-820 (2014).

60. Li N, *et al.* Resting-state functional connectivity predicts impulsivity in economic decision-making. *The Journal of neuroscience : the official journal of the Society for Neuroscience* **33**, 4886-4895 (2013).

61. Cools R, Clark L, Robbins TW. Differential responses in human striatum and prefrontal cortex to changes in object and rule relevance. *The Journal of neuroscience : the official journal of the Society for Neuroscience* **24**, 1129-1135 (2004).

62. Frank MJ, Badre D. Mechanisms of hierarchical reinforcement learning in corticostriatal circuits 1: computational analysis. *Cerebral cortex (New York, NY : 1991)* **22**, 509-526 (2012).

63. Chadick JZ, Gazzaley A. Differential coupling of visual cortex with default or frontal-parietal network based on goals. *Nature neuroscience* **14**, 830-832 (2011).

64. Gilmore AW, Nelson SM, McDermott KB. A parietal memory network revealed by multiple MRI methods. *Trends in cognitive sciences* **19**, 534-543 (2015).

65. Cohen MX. Neurocomputational mechanisms of reinforcement-guided learning in humans: A review. *Cognitive, Affective, & Behavioral Neuroscience* **8**, 113-125 (2008).

66. Sescousse G, Caldú X, Segura B, Dreher J-C. Processing of primary and secondary rewards: A quantitative meta-analysis and review of human functional neuroimaging studies. *Neuroscience & Biobehavioral Reviews* **37**, 681-696 (2013).

67. García-Cabezas MA, Martínez-Sánchez P, Sánchez-González MA, Garzón M, Cavada C. Dopamine innervation in the thalamus: monkey versus rat. *Cerebral cortex (New York, NY : 1991)* **19**, 424-434 (2009).

68. Sánchez-González MA, García-Cabezas MA, Rico B, Cavada C. The primate thalamus is a key target for brain dopamine. *The Journal of neuroscience : the official journal of the Society for Neuroscience* **25**, 6076-6083 (2005).

69. Lisman JE, Pi HJ, Zhang Y, Otmakhova NA. A thalamo-hippocampal-ventral tegmental area loop may produce the positive feedback that underlies the psychotic break in schizophrenia. *Biological psychiatry* **68**, 17-24 (2010).

70. Oke AF, Adams RN, Winblad B, von Knorring L. Elevated dopamine/norepinephrine ratios in thalami of schizophrenic brains. *Biological psychiatry* **24**, 79-82 (1988).

71. Takahashi H, Yamada M, Suhara T. Functional significance of central D1 receptors in cognition: beyond working memory. *Journal of cerebral blood flow and metabolism : official journal of the International Society of Cerebral Blood Flow and Metabolism* **32**, 1248-1258 (2012).

72. Sedvall GC, Karlsson P. Pharmacological Manipulation of D1-Dopamine Receptor Function in Schizophrenia. *Neuropsychopharmacology : official publication of the American College of Neuropsychopharmacology* **21**, S181-S188 (1999).

73. Yun S*, et al.* Antipsychotic drug efficacy correlates with the modulation of D1 rather than D2 receptor-expressing striatal projection neurons. *Nature neuroscience* **26**, 1417-1428 (2023).

74. Hwang J, Mitz AR, Murray EA. NIMH MonkeyLogic: Behavioral control and data acquisition in MATLAB. *Journal of neuroscience methods* **323**, 13-21 (2019).

75. Cox RW. AFNI: software for analysis and visualization of functional magnetic resonance neuroimages. *Computers and biomedical research, an international journal* **29**, 162-173 (1996).

76. Wang X*, et al.* U-net model for brain extraction: Trained on humans for transfer to non-human primates. *NeuroImage* **235**, 118001 (2021).

77. Seidlitz J*, et al.* A population MRI brain template and analysis tools for the macaque. *NeuroImage* **170**, 121-131 (2018).

78. Taylor PA, Saad ZS. FATCAT: (an efficient) Functional and Tractographic Connectivity Analysis Toolbox. *Brain connectivity* **3**, 523-535 (2013).

79. Kassebaum P. circularGraph (https://github.com/paul-kassebaum-mathworks/circularGraph), GitHub. . (2023).

Subject	*Behavior*	*SCH-rsMRI*	*HAL-rsMRI*	*Saline-rsMRI*
Ee	Y	Y	N	Y
Me	Y	N	Y	N
Pi	Y	Y	Y	Y
St	Y	Y	Y	N
Bu	N	N	N	Y
Cy	N	N	N	Y
Wo	N	N	N	Y

Table 1. Assignments of monkeys to resting-state fMRI and behavioral testing conditions. Y and N indicate the condition that the data was collected and not collected, respectively. SCH: SCH-23390 (10 µg/kg), HAL: haloperidol (50 µg/kg). Note that animals assigned to behavioral experiments (Ee, Me, Pi, St) went through all drug treatment conditions.

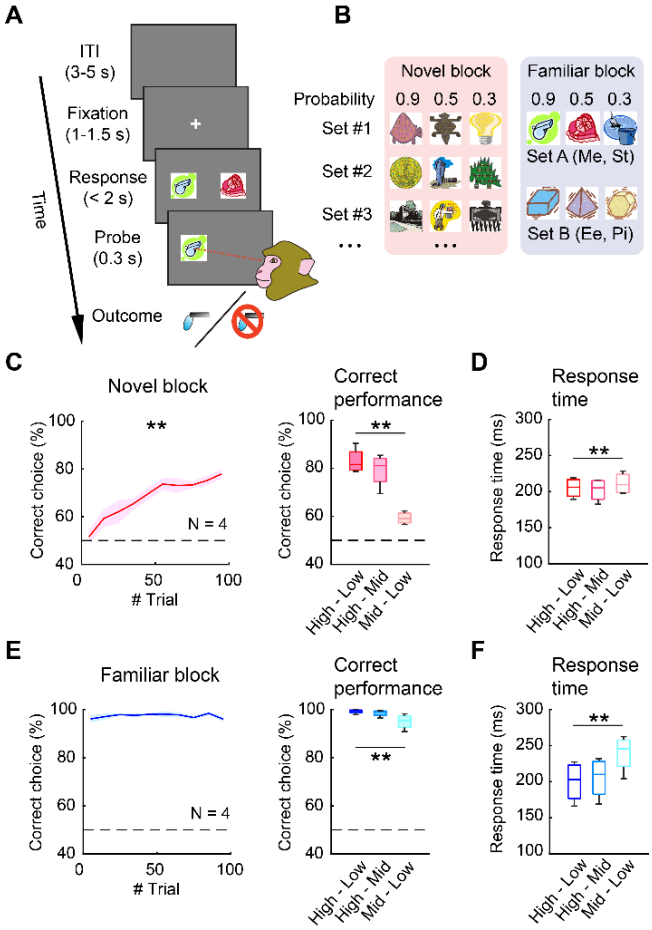

Figure 1. Behavioral task and baseline behavioral performance. (**A**) Trial sequence. Animals were required to respond to one of two visual stimuli on the screen by eye movement to acquire a drop of juice. (**B**) Stimulus sets. Stimuli were pictures that were associated with different reward probabilities (0.9, 0.5, 0.3). In novel blocks (left), a new set of three pictures was used in each block. In familiar blocks (right), a fixed set of pictures was prepared for each monkey and used repeatedly throughout the experiment. (**C**) Task performance in novel blocks. Correct performance was gradually increased over trials in a block (left) and depending on which stimuli were paired in the trial (right). Dashed lines indicate chance level, and the plots show mean and standard error. (**D**) Response time (RT) in novel blocks reflected reward probability of the stimulus pair. (**E and F**) Behaviors in familiar blocks. Correct performance was stable throughout the block. Performance and RT reflected reward probability. Conventions are the same as **C-D**. ** $p < 0.01$, interaction of trial bin by block type, 2-way repeated-measures ANOVA, or main effect of stimulus pair, 1-way repeated-measures ANOVA.

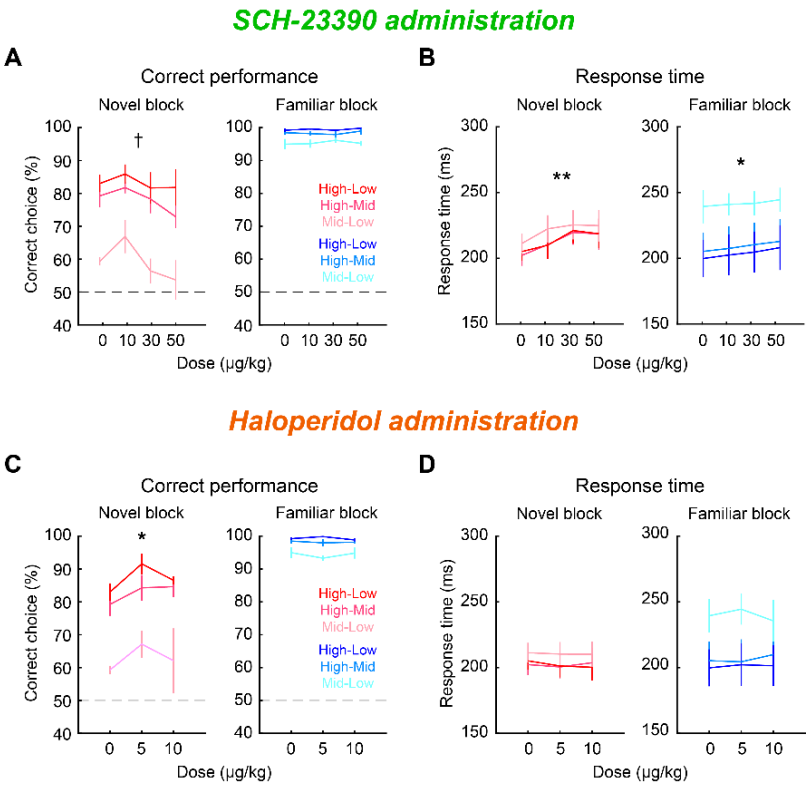

Figure 2. Effects of DA receptor antagonists on behaviors. (**A**) Task performance in SCH-23390 sessions. Correct performance tended to decrease when higher dose of SCH was administered in novel blocks (left) but did not change in familiar blocks (right). The colors of lines indicate stimulus pairs. (**B**) RT in SCH-23390 sessions. RT increased following SCH injection. (**C and D**) Haloperidol sessions. Conventions are the same as **A and B**. †$p < 0.10$, *$p < 0.05$, **$p < 0.01$, 2-way repeated-measures ANOVA.

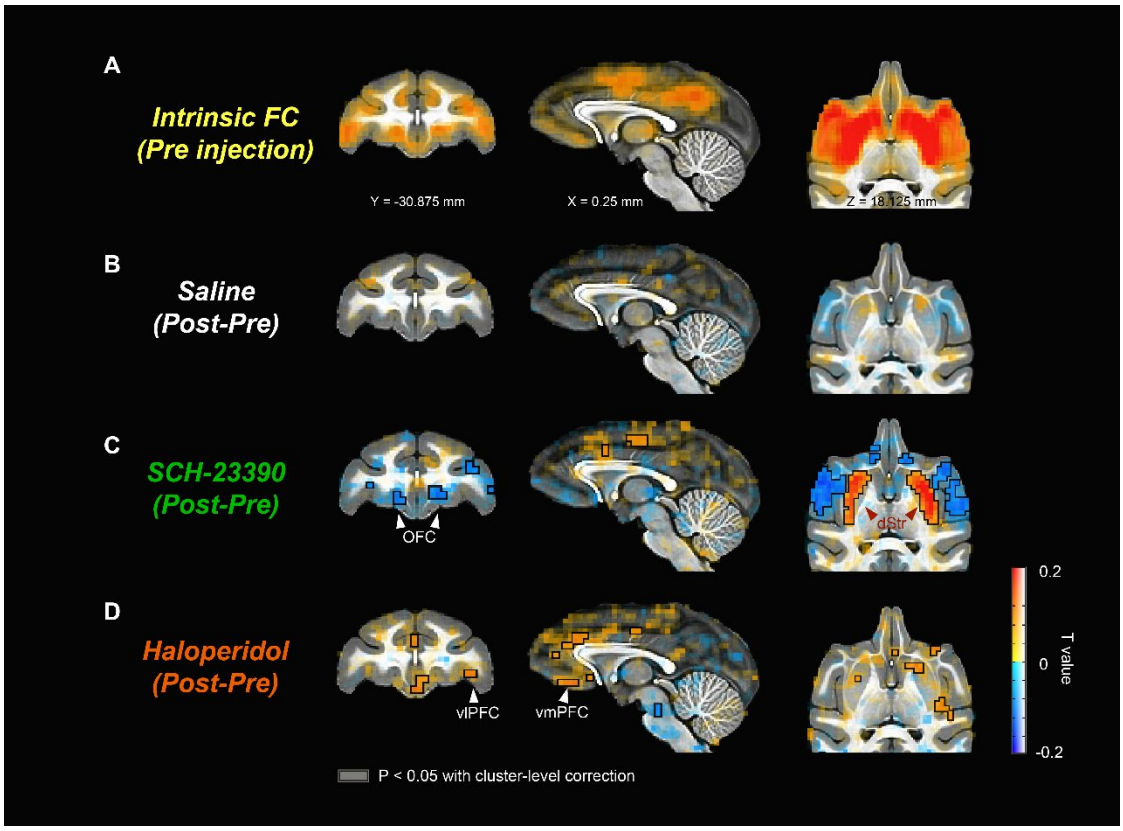

Figure 3. Functional connectivity analysis. (**A**) Whole-brain FC computed using dorsal striatum as ROI to pre-injection images. Coronal (left), sagittal (middle), and axial planes (right) are shown. Colors indicate strength of FC (T-value). (**B**) Changes in dorsal striatum FC from pre- to post-saline injection scans. (**C**) SCH-23390 effects on FC. (**D**) Haloperidol effects on FC. The voxels enclosed in black lines are the clusters with significant dorsal striatum FC ($p < 0.05$, cluster-level correction). dStr: dorsal striatum, OFC: orbitofrontal cortex, vlPFC: ventrolateral prefrontal cortex, vmPFC: ventromedial prefrontal cortex.

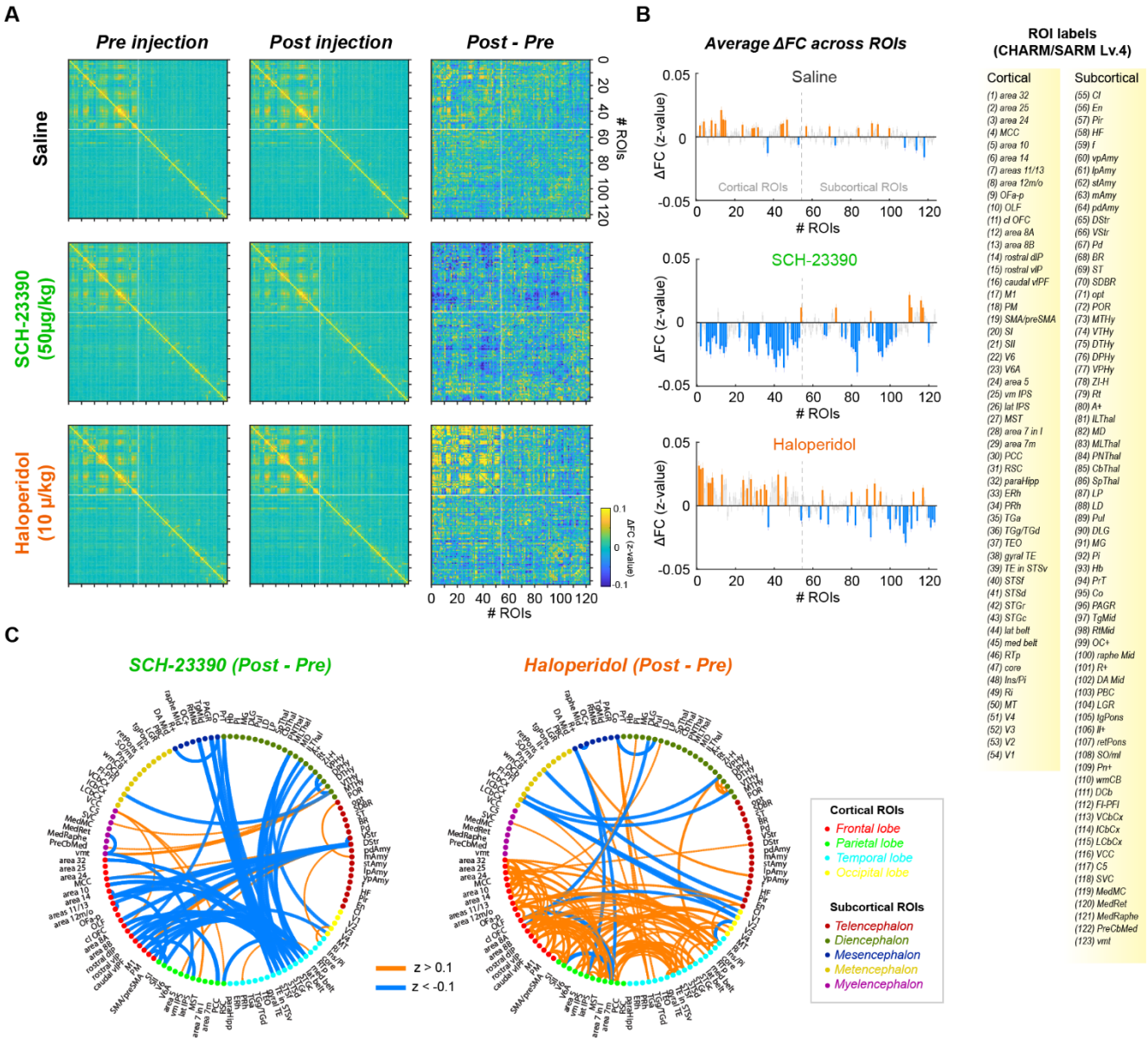

Figure 4. Connectome analysis. (**A**) Connectome for pre-injection (left), post-injection (middle), and their difference (ΔFC, right) are shown for sessions with injection of saline (top row), SCH-23390 (middle row), and haloperidol (bottom row), respectively. X and Y axes are the number of ROIs defined by macaque brain hierarchical atlas (CHARM/SARM atlas at level 4). Colors indicate the FC of each pair of ROIs (z-value). White lines on connectome divide cortical and subcortical ROIs. (**B**) Bar plots showing average ΔFC for saline (top), SCH-23390 (middle), and haloperidol (bottom) sessions. ΔFC (z-value) is averaged for each ROI. Orange and blue bars indicate significant ΔFC from zero ($p < 0.05$, Bonferroni correction). Dashed lines divide cortical and subcortical ROIs. ROI labels from CHARM/SARM level 4 are shown on the right. (**C**) Circular plots depicting the effects of injection of SCH-23390 (left) or haloperidol (right) on the whole-brain FC. Seed region labels correspond to ROI labels in **B**. The changes in FC are indicated by color (orange: positive changes, blue: negative changes) and width of lines (absolute z-value changes > 0.1). The color of each seed indicates the region defined by CHARM/SARM level 1 (inset).

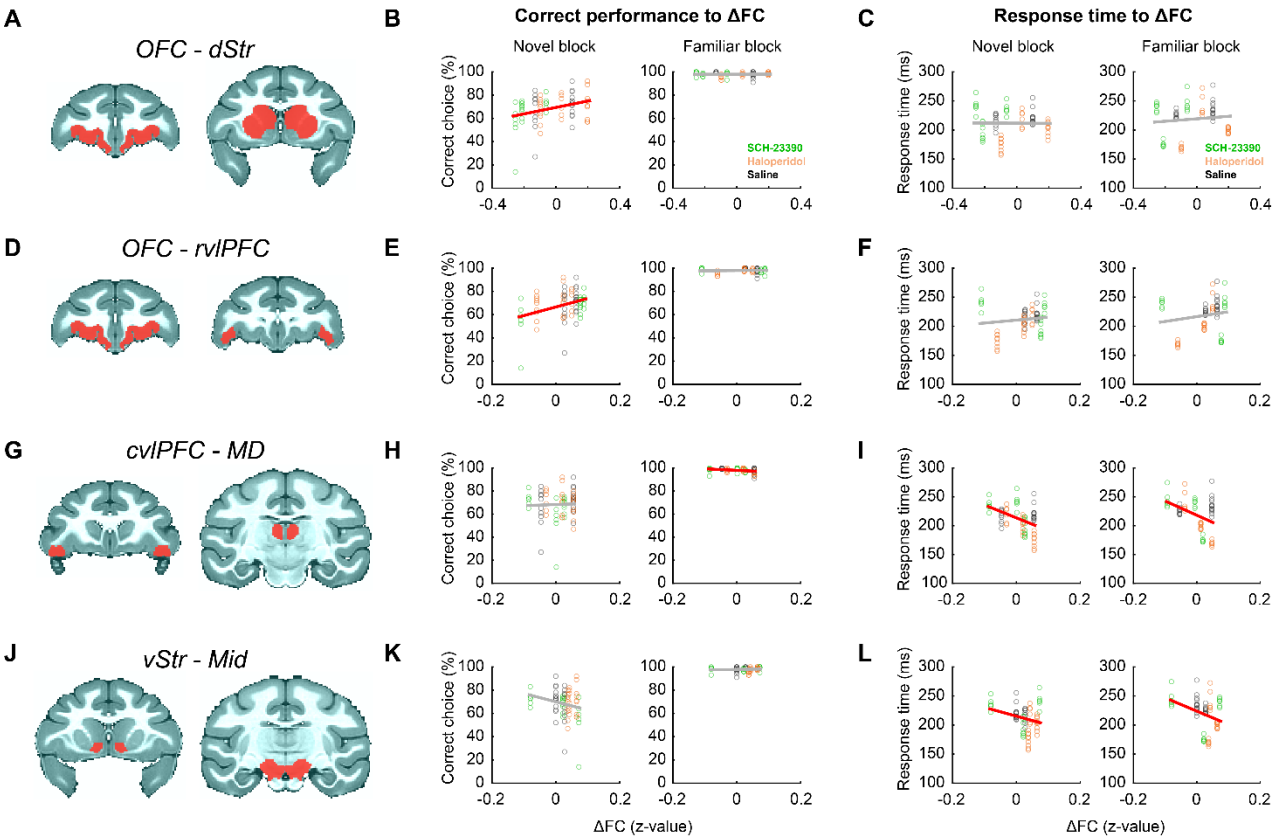

Figure 5. Direct comparison of behaviors and resting-state FC. (**A-C**) Correlation between orbitofrontal cortex to dorsal striatum FC and task performance in novel (left) and familiar (right) blocks (**B**) or response time (**C**). Red areas in brain map show bilateral ROIs. Plots indicate behavioral data and corresponding ΔFC in saline (black), SCH-23390 (green), and haloperidol (orange) sessions. Red and gray lines on scatter plots indicate significant ($p < 0.05$, linear regression analysis) and non-significant relationships between behavior and ΔFC, respectively. (**D-F**) Correlation between orbitofrontal cortex to rostral part of ventrolateral prefrontal cortex FC and behaviors. (**G-I**) Correlation between the caudal part of ventrolateral prefrontal cortex to mediodorsal thalamus FC and behaviors. (**J-L**) Correlation between ventral striatum to midbrain FC and behaviors. Conventions are the same as **A-C**.

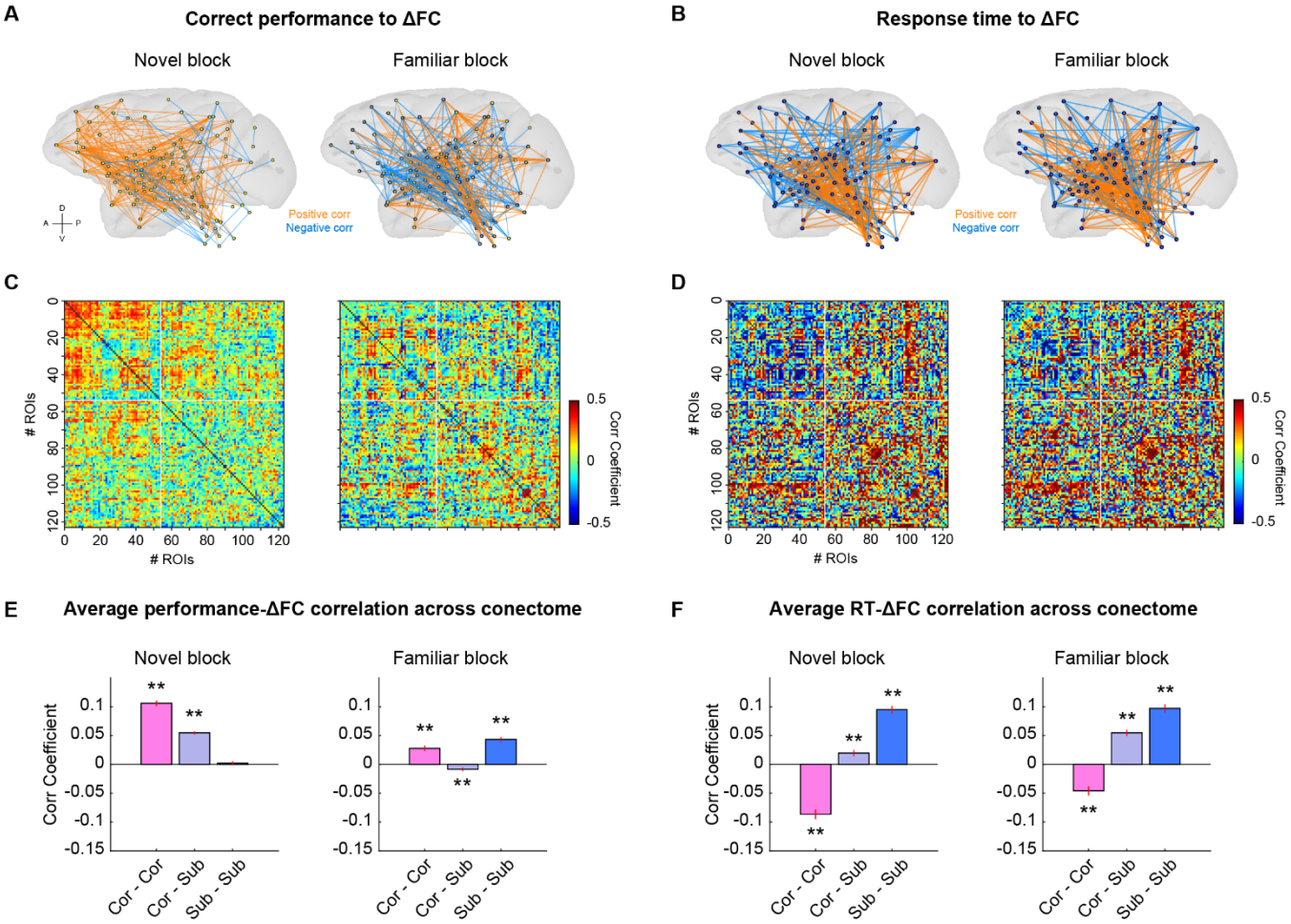

Figure 6. Whole-brain network correlation to behaviors across all drug conditions. (**A**) Strength of performance-ΔFC correlation projected into brain map. The top 5% of connections that showed strong behavior-ΔFC correlation are visualized. Black dots indicate the center of mass of ROIs. The strength and direction of changes in FC are depicted as the width and color (orange: positive, blue: negative) of lines, respectively. (**B**) Strength of RT-ΔFC correlation projected into brain map. (**C**) Correlation matrix depicting relationship between changes in FC and task performance in novel (left) and familiar (right) blocks. The ROIs used are the same as in **Fig. 4A**. Colors indicate performance-ΔFC correlation coefficient. (**D**) Correlation between changes in FC and RT. (**E**) Bar plots depicting average performance-ΔFC correlation coefficients calculated for cortico-cortical, cortico-subcortical, and subcortico-subcortical connections separately, in novel (left panel) and familiar (right panel) blocks. (**F**) Averaged correlation coefficients for RT to ΔFC. **$p < 0.01$, rank-sum test.